Available online at www.sciencedirect.com
SCIENCE DIRECT
Journal of Catalysis 237 (2006) 381–392
JOURNAL OF CATALYSIS
www.elsevier.com/locate/jcat

Selective catalytic reduction of nitric oxide with hydrogen over Pd-based catalysts

Gongshin Qi [a], Ralph T. Yang [a,*], Fabrizio C. Rinaldi [b]

[a] *Department of Chemical Engineering, University of Michigan, Ann Arbor, MI 48109-2136, USA*
[b] *Tenneco Automotive, Exhaust Engineering Center, Grass Lake, MI 49240, USA*

Received 12 September 2005; revised 14 November 2005; accepted 21 November 2005

Abstract

Catalytic reduction of NO with hydrogen in the presence of excess oxygen was studied using Pd-based catalysts. High steady-state conversion of NO (>80%) is achieved, using 1%Pd/TiO_2/Al_2O_3 as the catalyst and at temperatures ranging from 140 to 180 °C. The addition of V_2O_5 to this catalyst not only increases NO conversion, but also widens the reaction temperature window to 250 °C. The effects of CO, O_2, and H_2 concentrations on the NO conversion were also investigated. It was found that the reaction order is nearly first order with respect to NO, 0.6 with respect to H_2 and −0.18 with respect to CO. Increasing the O_2 concentration from 2 to 10% produced only a slight decrease in NO conversion. FTIR studies showed that a significant amount of NH_4^+ was formed over the V_2O_5-containing catalyst, during the reaction, at temperatures >200 °C, compared with almost no NH_4^+ formation over the V_2O_5-free sample. The higher activity of 1%Pd–5%V_2O_5/TiO_2–Al_2O_3 is partly attributed to the in situ formation of NH_4^+.

Keywords: NO_x reduction by hydrogen; Selective catalytic reduction of NO; Diesel engines; Pd-based catalysts; Lean burn engines; Pd–V_2O_5/TiO_2–Al_2O_3

1. Introduction

Nitrogen oxides (NO, NO_2, and N_2O) resulting from combustion processes continue to be a major source of air pollution. They contribute to photochemical smog, acid rain, ozone depletion, ground-level ozone, and greenhouse effects. More than 95% of NO_x emissions are derived from two sources, ∼49% from mobile (vehicles) and ∼46% from stationary (power plants) [1]. Currently the commercially available technology for reducing NO_x ($x = 1, 2$) emissions from stationary sources is selective catalytic reduction (SCR). Ammonia is widely accepted as the reducing agent of choice. Many catalyst formulations have been reported to be active for this reaction. These can be subdivided into two main groups, mixed oxides and ion-exchanged molecular sieves [2,3]. Commercially available catalyst formulations contain, among others, vanadia (doped with MoO_3 or WO_3) supported on titania.

Similar SCR technology also has been effectively applied to mobile sources, where ammonia is usually generated by the thermal decomposition of urea. However, there are some commercial and logistic drawbacks, namely (1) a separate tank and injection system, (2) issues relating to NH_3 slip (i.e., unreacted ammonia), (3) handling of urea solutions during cold conditions, and (4) as of yet, no real infrastructure to widely deploy the needed urea solution. These factors indicate that the development of an active NO_x, reduction catalyst that makes use of other reductants is desirable. Three-way catalysis is very effective on emissions from gasoline engines, where narrow-band oxygen sensors afford a tight closed-loop control of the air:fuel ratio (∼14.7). In comparison, diesel engines operate very lean and with a wider band of air:fuel ratio (14–24) [4]. Diesel engines have considerable benefits over gasoline engines, including better fuel economy, less CO_2 production, higher torque, cooler exhaust temperatures, and overall greater longevity [4]. However, due to the nature of diesel fuel and of the compression ignition combustion process, diesel engines emit a high quantity of particulate matter (PM) and NO_x emissions. These pose a significant air quality issue, accounting for about one-

* Corresponding author. Fax: +1 734 763 0459.
E-mail address: yang@umich.edu (R.T. Yang).

0021-9517/$ – see front matter
doi:10.1016/j.jcat.2005.11.025

third of the nation's NO_x emissions and one-quarter of the PM emissions from mobile sources. In the United States, the Environmental Protection Agency (EPA) has addressed such concerns by imposing increasingly stringent emission regulations, the latest wave of which are Tier 2 for light duty vehicles and both the 2004 Rule and 2010 Highway Rule for heavy-duty diesel engines (all mobile, on-road applications). Due to these stringent emission regulations, urea SCR has received renewed attention as an NO_x abatement tool for mobile sources [5–7], together with NO_x traps and exhaust gas recirculation (EGR). Although urea-SCR is very effective and has high N_2 selectivity, the earlier-mentioned drawbacks remain.

Recently, hydrogen has been used in an effort to regenerate effectively NO_x traps. Its long-term prospects (fueling internal combustion engines, fuel cell vehicles, on-board reforming of diesel fuel, producing essentially only water vapor) make hydrogen the most likely candidate as a reductant in a SCR reaction to abate NO_x emissions in an excess oxygen environment, such as diesel engine exhaust. The following main reactions occur in the $NO/H_2/O_2$ system:

$$2NO + 4H_2 + O_2 \rightarrow N_2 + 4H_2O,$$

$$2NO + 3H_2 + O_2 \rightarrow N_2O + 3H_2O,$$

$$O_2 + 2H_2 \rightarrow 2H_2O.$$

A number of groups have investigated the use of hydrogen as a reductant over Pt-based catalysts [8–12]. Yokota et al. [8] investigated NO reduction with H_2 and CO in the presence of excess oxygen and found that the Pt/zeolite catalyst has high activity with a N_2 selectivity of 50%. An improved catalyst, Pt–Mo–Na/SiO_2, also developed by Yokota et al. [8], has a wider temperature window for NO_x conversion and a lower selectivity to the byproduct, N_2O, than the conventional Pt catalysts. Burch and Coleman [11] investigated NO reduction with H_2 in the presence of excess oxygen over Pt/SiO_2 and Pt/Al_2O_3 catalysts and found the SiO_2 supported catalysts to be more active at lower temperatures than the Al_2O_3-supported catalyst. Costa et al. [12] reported an improved Pt-based catalyst with the use of mixed-oxide $La_{0.5}Ce_{0.5}MnO_3$ supports. The improved catalyst performance was attributed to the presence of oxygen vacancies on the support surface adjacent to small platinum clusters. These oxygen vacancies were thought to participate in the reaction mechanism. Ueda et al. [10] investigated the $H_2/NO/O_2$ reaction on Pt- and Pd-based catalysts and found two conversion maxima at 373 and 573 K in the reduction of NO with H_2 over supported Pd catalysts. The appearance of two conversion maxima can be explained by a switch in the reaction pathways: direct reduction of NO by H_2 at approximately 373 K and reduction of in situ generated NO_2 by H_2 at approximately 573 K. Lee and Gulari [18] studied H_2-SCR in the presence of CO on Pd/Al_2O_3 prepared by $PdCl_2$ as a precursor and found it to be more active than Pd/Al_2O_3 prepared by $Pd(NO_3)_2$ as a precursor. More recently, Nanba et al. [19] investigated the reduction of NO by H_2 in the presence of O_2 over physical mixtures of Pt/ZrO_2 and secondary catalysts active for the SCR of NO by ammonia.

In summary, hydrogen has proven to be a promising reductant for NO under lean burn conditions over Pt- and Pd-based catalysts. H_2 is available from fuel processors for fuel cell applications. Moreover, CO is available both within raw diesel engine exhaust and as part of a reformation process. Because it bonds strongly to catalysts, CO could have a significantly detrimental effect on the low-temperature oxidation of H_2 by both NO and O_2 [13–15]. Macleod and Lambert [16] investigated the influence of CO on both the activity and selectivity of Pt- and Pd-based catalysts and showed that for the Pt catalysts, the presence of CO did indeed have a significantly detrimental effect. Macleod and Lambert [17] reported a highly active Pd/TiO_2/Al_2O_3 catalyst capable of >90% NO conversion (at a high space velocity) in the presence of excess oxygen at 140–180 °C with N_2 selectivity up to 80%. This catalyst would not be suitable in a diesel engine exhaust stream, because a wider operating temperature window is required.

The objective of this work is to investigate and develop SCR catalyst formulations that use hydrogen as the reducing agent and can lower the NO_x content of a 2004-compliant heavy-duty engine exhaust to the 2010 Highway Rule levels. The catalyst developed in this work must have high activity and a wider temperature window than previously developed catalysts, both of which are critical for practical applications. Another aspect of our study is steady-state reactions, as opposed to the transient reactions studied by others, such as Macleod and Lambert [17]. We also aim to clarify the function and role of V_2O_5 in the Pd-based catalysts.

2. Experimental

2.1. Preparation of catalysts

The 20 wt%TiO_2-on-γ-Al_2O_3 support was prepared by hydrolysis of a solution of $Ti[O(CH_2)_3CH_3]_4$ in the presence of γ-Al_2O_3 (PSD-350 grade, BET surface area approximately 350 m^2/g, 60–100 mesh; Alcoa). The solid sample was then dried in air at 500 °C for 6 h. The 5%V_2O_5/20 wt%TiO_2-γ-Al_2O_3 was prepared by impregnation in 20%TiO_2-γ-Al_2O_3 with an aqueous solution of NH_4VO_3 in oxalic acid. The same procedure was used to prepare 5%V_2O_5/Al_2O_3 and 5%V_2O_5/TiO_2 (P25, Degussa, BET surface area = 30.6 m^2/g). After impregnation, these catalysts were dried at 120 °C for 12 h, then calcined at 500 °C in oxygen for 12 h to decompose the ammonium salt into the corresponding oxide. Palladium was subsequently impregnated in 5%V_2O_5/20 wt%TiO_2-γ-Al_2O_3 and 20wt%TiO_2-γ-Al_2O_3 using a $Pd(NH_3)_4Cl_2$ aqueous solution. The catalyst was then dried at 120 °C for 12 h and calcined at 500 °C for 6 h in oxygen.

2.2. Catalytic activity measurement

The activity measurement was carried out in a fixed-bed quartz reactor. The typical reactant gas composition was 500 ppm NO, 4000 ppm H_2, 0–2000 ppm CO (when used), 5% O_2, and the balance He. A 100-mg sample was used in each run. The total flow rate was 200 ml/min (under ambient conditions). The premixed gases (1.01% NO in He, 5.00% H_2 in He, and 1.0% CO in He) were supplied by Matheson. Water vapor

was generated by passing He through a heated saturator containing deionized water. The NO and NO_2 concentrations were continually monitored using a chemiluminescent NO/NO_x analyzer (Thermo Environmental Instruments model 42C). The products were analyzed using a gas chromatograph (Shimadzu model 8A) with a 13X molecular sieve column for H_2, CO, and N_2 separation and a Porapak Q column for N_2O. Ammonia formation was monitored by FTIR. In no case was ammonia detected by FTIR under lean burn conditions, consistent with the report by Shelef et al. [20]. The catalytic activity was based on the calculated NO_x (NO + NO_2) conversion using the following formula:

$$NO_x \text{ conversion} = \frac{\text{inlet } NO_x\,(\text{ppm}) - \text{outlet } NO_x\,(\text{ppm})}{\text{inlet } NO_x\,(\text{ppm})} \times 100\ (\%).$$

The N_2 selectivity was calculated as follows:

$$N_2 \text{ selectivity} = \frac{[N_2]}{[N_2] + [N_2O]} \times 100\ (\%).$$

Because the reactions were carried out at relatively low temperature, part of the decrease in NO concentration could be attributed to the adsorption of NO onto the catalysts. Thus, to ensure that this did not occur, at the beginning of each experiment the catalyst was purged with reactant gas until the inlet and outlet NO concentrations were equal (i.e., 500 ppm). Subsequently, the temperature was raised to the desired level. At each reaction temperature, NO conversion and product analysis was performed after allowing the reaction to reach steady state (usually 1–2 h, depending on the reaction).

The nitrogen balance was calculated for each step using the following equation: inlet [NO] = outlet {[NO] + 2[N_2] + 2[N_2O]}. This was found to be >95% for all experiments.

Steady-state kinetic studies for the NO reduction by H_2 in the presence of CO and O_2 were also carried out for the 1%Pd–5%V_2O_5/TiO_2/Al_2O_3 catalyst, using a fixed-bed quartz flow reactor, with 5 mg of catalyst used in each run. The NO concentration in an exhaust was simulated by blending different gaseous reactants. The typical reactant gas composition was 0–5000 ppm H_2, 100–500 ppm NO, 0–500 ppm CO, 1–5% O_2, and the balance He. The total flow rate was 500 ml/min (under ambient conditions). The same instrumentation as described above was used throughout.

2.3. Catalyst characterization

Powder X-ray diffraction (XRD) measurements were carried out on the catalysts using a Rigaku Rotaflex D/Max-C system with a Cu-K_α ($\lambda = 0.1543$ nm) radiation source. The samples were loaded with a depth of 1 mm.

In each H_2 temperature-programmed reduction (TPR) experiment, 50 mg of sample was loaded into a quartz reactor and then pretreated with O_2/He (100 ml/min) flow at 500 °C for 0.5 h. The sample was then cooled to room temperature in an O_2/He flow. Sample reduction was carried out starting at room temperature to 600 °C in a 5.32%H_2/N_2 flow (40 ml/min) with a temperature ramp of 10 °C/min. The consumption of H_2 was monitored using a thermal conductivity detector. The water produced during the reduction was trapped in a 5-Å molecular sieve column.

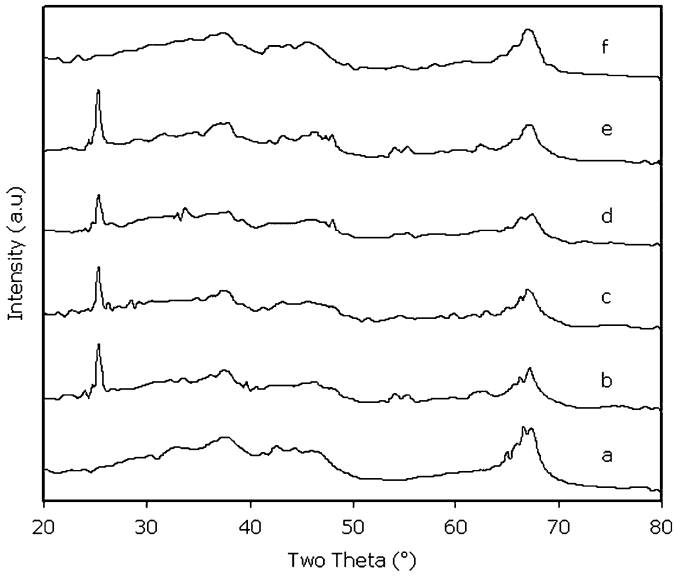

Fig. 1. XRD patterns of the catalysts: (a) Al_2O_3, (b) 20%TiO_2/Al_2O_3, (c) 5%V_2O_5/20%TiO_2/Al_2O_3, (d) 1%Pd–5%V_2O_5/TiO_2/Al_2O_3, (e) 1%Pd/20%TiO_2/Al_2O_3, (f) 1%Pd–5%V_2O_5/Al_2O_3.

Infrared spectra were recorded on a Nicolet Impact 400 FTIR spectrometer with a TGS detector. The sample was prepared as a self-supporting wafer 1.3 cm in diameter. This was achieved by compressing 15 mg of the sample. The wafer was then loaded into the IR cell (BaF_2 windows). The wafers were pretreated at 573 K in a flow of high-purity O_2/He for 0.5 h, then cooled to room temperature. At each temperature step, the background spectrum was recorded in flowing O_2/He. This spectrum was subsequently subtracted from the sample spectrum obtained at the same temperature step. Thus the IR absorption features that originated from the structure vibrations of the catalyst were eliminated from the sample spectra. IR spectra were recorded by accumulating 100 scans at a spectra resolution of 4 cm^{-1}.

3. Results

3.1. Characterization of catalysts

The XRD patterns of the catalysts are shown in Fig. 1. Crystalline PdO phases were not detected in any samples, indicating that Pd was highly dispersed on the support. Four diffraction peaks with $2\theta = 25.3, 37.5, 39.4$, and 48 were observed in the titania-containing samples. These peaks originated from the anatase form of titania.

H_2-TPR profiles of the 1%Pd–5%V_2O_5/TiO_2–Al_2O_3 and 1%Pd/TiO_2–Al_2O_3 catalysts are shown in Fig. 2. All samples demonstrate one main peak, which can be assigned to the reduction of Pd (II) to Pd(0). The reduction peak temperature is 46 °C higher on the V_2O_5-containing sample than on the V_2O_5-free sample. It is believed that V_2O_5 retards the reduction of Pd oxides.

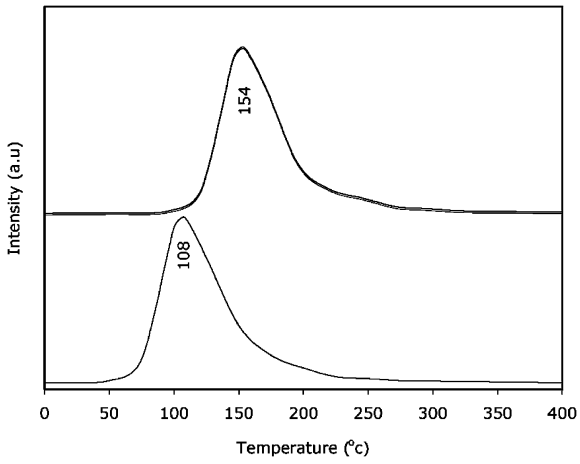

Fig. 2. TPR profiles of 1%Pd–5%V_2O_5/TiO_2/Al_2O_3 (upper) and 1%Pd/TiO_2/Al_2O_3 catalysts (lower).

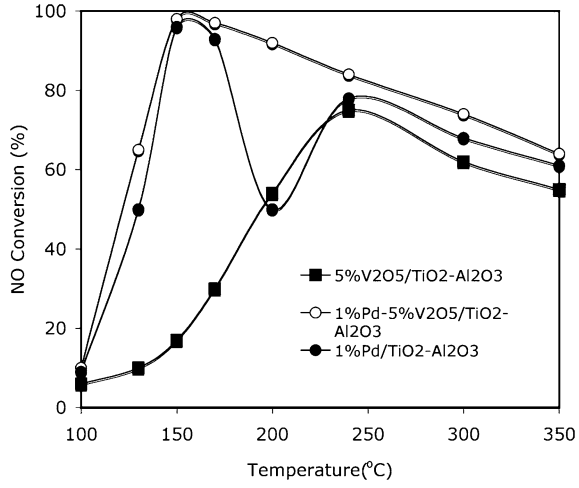

Fig. 3. NO conversion as a function of temperature over various catalysts. Reaction conditions: 0.1 g catalyst, total flow rate = 200 ml/min, [NO] = 500 ppm, [O_2] = 5%, [H_2] = 4000 ppm, He = balance.

3.2. NO_x reduction on Pd-based catalysts by H_2 in the presence of oxygen

The performance of a range of Pd-based catalysts is shown in Fig. 3. A maximum NO conversion of 98% was achieved at 150 °C over the 1%Pd–5%V_2O_5/TiO_2/Al_2O_3 catalyst. This reaction displayed only one NO conversion peak. Under the same conditions, the 1%Pd/TiO_2/Al_2O_3 catalyst also showed high NO conversion. However, two separated NO conversion peaks at 150 and 240 °C were observed. These findings are consistent with the reports of Ueda et al. [10] and Macleod and Lambert [16,17]. Whereas a maximum NO conversion of 80% was obtained over the 5%V_2O_5/TiO_2/Al_2O_3 catalyst, the peak conversion temperature was the same as the second NO conversion peak for the 1%Pd/TiO_2/Al_2O_3 catalyst. This could indicate that the second NO conversion peak may not depend on the Pd concentration. Fig. 3 shows that adding V_2O_5 to the 1%Pd/TiO_2/Al_2O_3 catalyst increased the NO conversion, especially at temperatures around 200 °C. Thus

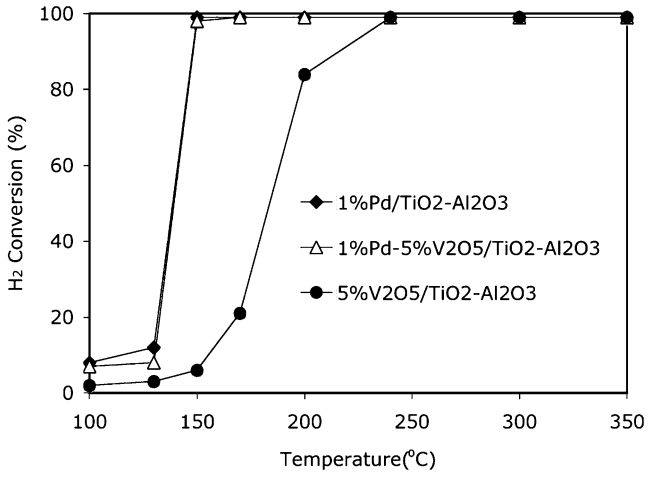

Fig. 4. H_2 conversion as a function of temperature over various catalysts. Reaction conditions: 0.1 g catalyst, total flow rate = 200 ml/min, [NO] = 500 ppm, [O_2] = 5%, [H_2] = 4000 ppm, He = balance.

the addition of V_2O_5 widens the high NO conversion temperature window to 140–250 °C (80% NO conversion). The 1%Pd/TiO_2/Al_2O_3 catalyst exhibited a narrower NO conversion temperature window of 140–180 °C. The NO conversion order was 1%Pd–5%V_2O_5/TiO_2/Al_2O_3 > 1%Pd/TiO_2/Al_2O_3 > 5%V_2O_5/TiO_2/Al_2O_3, based on the investigated temperature range.

Hydrogen conversions as a function of temperature on various TiO_2/Al_2O_3 supported catalysts are shown in Fig. 4. The H_2 conversion for each catalyst reached 100% at the temperatures where the maximum NO conversion was observed; on the 1%Pd/TiO_2/Al_2O_3 catalyst, this was achieved at 150 °C. In contrast, on the 1%Pd–5%V_2O_5/TiO_2/Al_2O_3 catalyst, 98% H_2 conversion was reached at 150 °C. The 5%V_2O_5/TiO_2/Al_2O_3 catalyst, on the other hand, reached complete H_2 conversion only at 240 °C.

For the best catalyst, 1%Pd–5%V_2O_5/TiO_2/Al_2O_3, Fig. 5 shows the NO–H_2–O_2 reaction activities, including NO conversion, H_2 conversion, and N_2 selectivity, at various space velocities. Generally, the space velocity significantly influenced the low-temperature NO conversion but not the high-temperature NO conversion. As the space velocity was increased (from 1.0×10^5 to 1.8×10^6 h^{-1}), NO conversion decreased, and maximum conversion shifted toward higher temperatures (150–200 °C). H_2 conversion exhibited a similar trend—namely, as the space velocity increased, H_2 conversion decreased. The corresponding 100% H_2 conversion temperature also increased. No significant space velocity effects were visible on the N_2 selectivity at temperatures below 200 °C. Significantly decreased N_2 selectivity was observed in the temperature range 200–300 °C.

Fig. 6 shows the conversions of NO and H_2 as well as the N_2 selectivity of various supported Pd catalysts as a function of temperature. It can be seen that at low temperatures (<170 °C), the 1%Pd–5%V_2O_5/TiO_2 catalyst had a very low activity, whereas 1%Pd–5%V_2O_5/TiO_2/Al_2O_3 catalyst and 1%Pd–5%V_2O_5/Al_2O_3 catalyst displayed relatively high activity under the same conditions. In the high-temperature

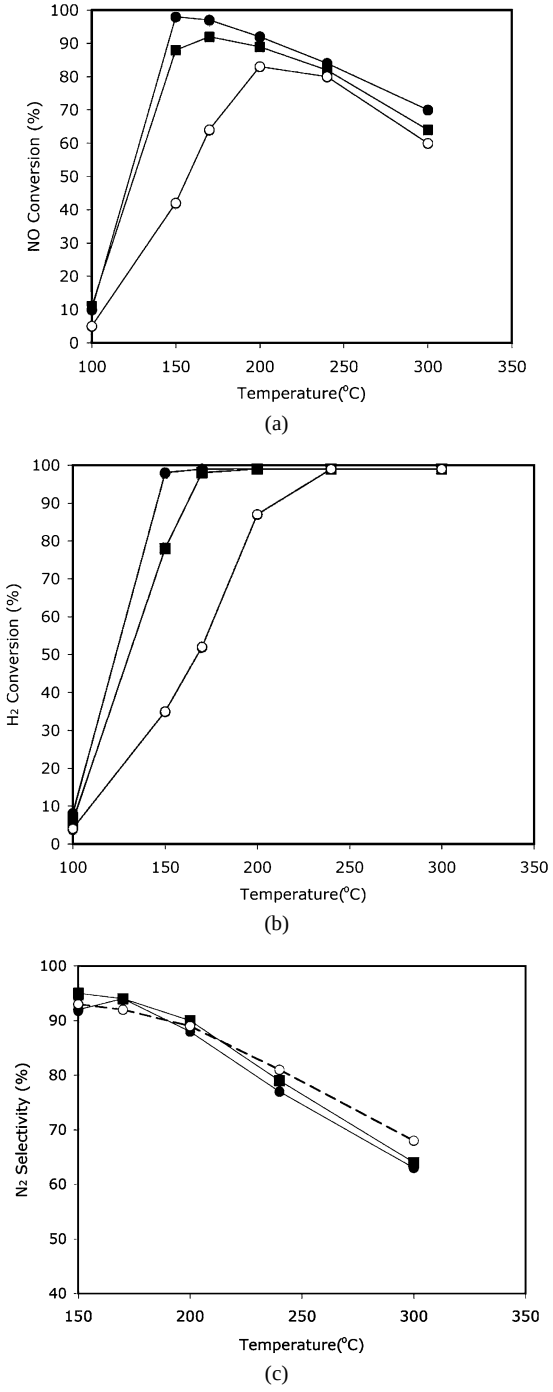

Fig. 5. Effect of space velocity on NO (a), H_2 conversions (b), and N_2 selectivity (c), for H_2-SCR over 1%Pd–5%V_2O_5/TiO_2/Al_2O_3 catalyst: ●, 1.0×10^5 h^{-1}; ■, 5.2×10^5 h^{-1}; ○, 1.8×10^6 h^{-1}. Reaction conditions: [NO] = 500 ppm, [H_2] = 4000 ppm, [O_2] = 5%, He = balance.

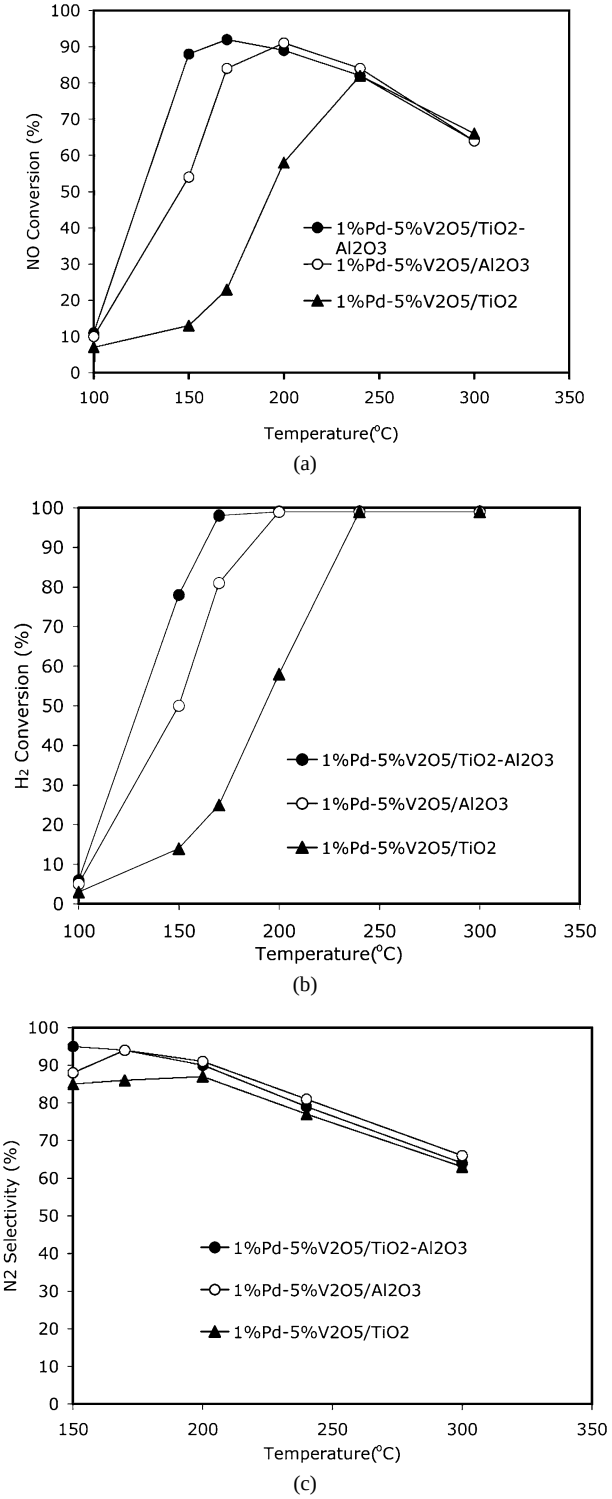

Fig. 6. NO (a), H_2 conversions (b), and N_2 selectivity (c), as functions of temperature over various supported Pd based catalysts. Reaction conditions: 0.05 g catalyst, [NO] = 500 ppm, [H_2] = 4000 ppm, [O_2] = 5%, He = balance, total flow rate = 500 ml/min.

range (>240 °C), all of the samples showed similar activity. The order of increasing activity of these Pd-based catalysts was 1%Pd–5%V_2O_5/TiO_2/Al_2O_3 > 1%Pd–5%V_2O_5/Al_2O_3 > 1%Pd–5%V_2O_5/TiO_2. The same trend was observed for H_2 conversion. Fig. 6 also shows the N_2 selectivity of different catalysts; all samples had a similar N_2 selectivity.

Fig. 7 displays NO conversions as a function of reaction time for catalysts 1%Pd–5%V_2O_5/Al_2O_3 (at 150 and 170 °C) and 1%Pd–5%V_2O_5/TiO_2–Al_2O_3 (at 150 °C). At 150 °C, the 1%Pd–5%V_2O_5/TiO_2–Al_2O_3 catalyst had a high NO conversion rate to reach steady state in only 1 h. A similar trend was observed for the 1%Pd–5%V_2O_5/Al_2O_3 catalyst at 170 °C. At 150 °C, however, the 1%Pd–5%V_2O_5/Al_2O_3 catalyst displayed

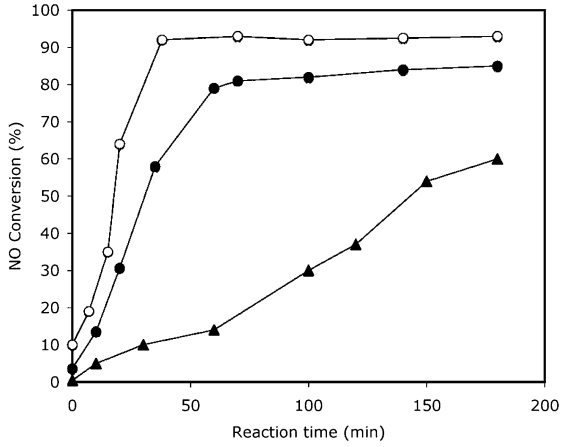

Fig. 7. NO conversion as a function of time on stream at 170 °C over 1%Pd–5%V_2O_5/Al_2O_3 (●), at 150 °C over 1%Pd–5%V_2O_5/Al_2O_3 (▲), and 1%Pd–5%V_2O_5/TiO_2–Al_2O_3 (○) catalysts for H_2-SCR. Reaction conditions: 0.05 g catalyst, [NO] = 500 ppm, [H_2] = 4000 ppm, [O_2] = 5%, He = balance, total flow rate = 500 ml/min.

a slow increase in NO conversion and reached only 60% NO conversion after 3 h. The 1%Pd–5%V_2O_5/TiO_2–Al_2O_3 catalyst had a higher conversion rate; thus it can be concluded that modification of Al_2O_3 by titania had a positive effect on the catalyst conversion rates. Fig. 7 also demonstrates that the H_2-SCR reaction needs to be studied after it has reached steady state and that transient study results must be interpreted with caution.

3.3. NO_x reduction on Pd-based catalysts by H_2 + CO in the presence of oxygen

The presence of CO in diesel engine exhaust gas prompted an investigation of the effects of CO on the H_2-SCR process. Fig. 8 shows the influence of CO on the H_2-SCR reaction over the 1%Pd–5%V_2O_5/TiO_2–Al_2O_3 catalyst with the total reductant concentration at 4000 ppm. Clearly, the presence of CO actually decreased NO conversion, especially in the low-temperature range. This result was different from that reported by Macleod and Lambert [16,17], who observed enhancement by CO on Pd/TiO_2/Al_2O_3. As the CO concentration was increased, the temperature of maximum NO conversion shifted from 150 to 200 °C. The presence of CO clearly inhibited the H_2 oxidation reaction, because the temperature to reach complete oxidation of H_2 increased from 170 to 200 °C as CO was added to the feed gas. In the low-temperature range, CO has a complex effect on N_2 selectivity, whereas at high temperatures, N_2 selectivity was almost independent of the presence of CO.

3.4. Kinetics studies for H_2-SCR in the presence of CO and excess O_2 in a differential reactor

To determine the reaction order with respect to NO, the concentrations of H_2, CO, and O_2 were kept constant while the concentration of NO was varied from 100 to 500 ppm. Similarly, to determine the reaction order with respect to H_2, the concentration of NO and CO were kept constant while the

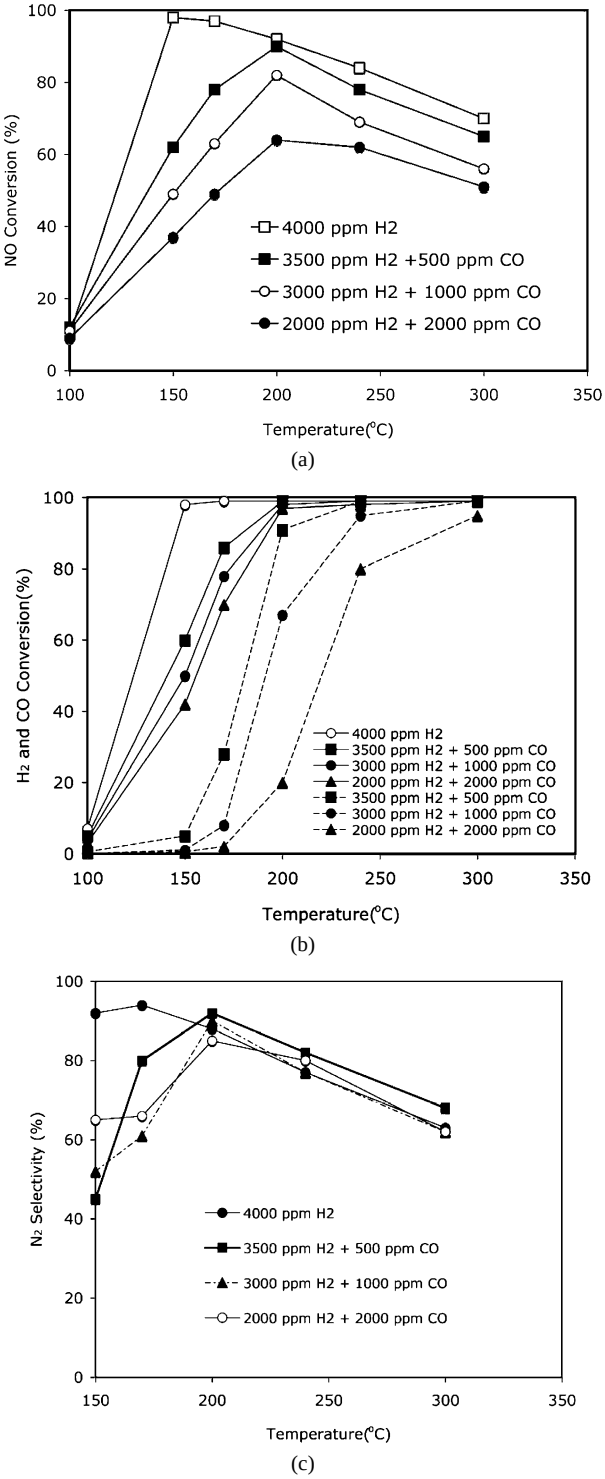

Fig. 8. NO (a), H_2, CO conversions (b) and N_2 selectivity (c) as functions of temperature over 1%Pd–5%V_2O_5/TiO_2–Al_2O_3 catalyst on different feed compositions. H_2 conversion (solid line), CO conversion (dashed line). Reaction conditions: 0.1 g catalyst, total flow rate = 200 ml/min, [NO] = 500 ppm, [O_2] = 5%, [H_2] = 2000–4000 ppm, [CO] = 0–2000 ppm, He = balance.

concentration of H_2 was varied between 1000 and 5000 ppm. Because the flow rate was 500 ml/min and only 5 mg of catalyst was used, <20% NO conversion was obtained at 200 °C in these experiments. Therefore, the reactor can be treated as a differential reactor. The experimental results on the rate of

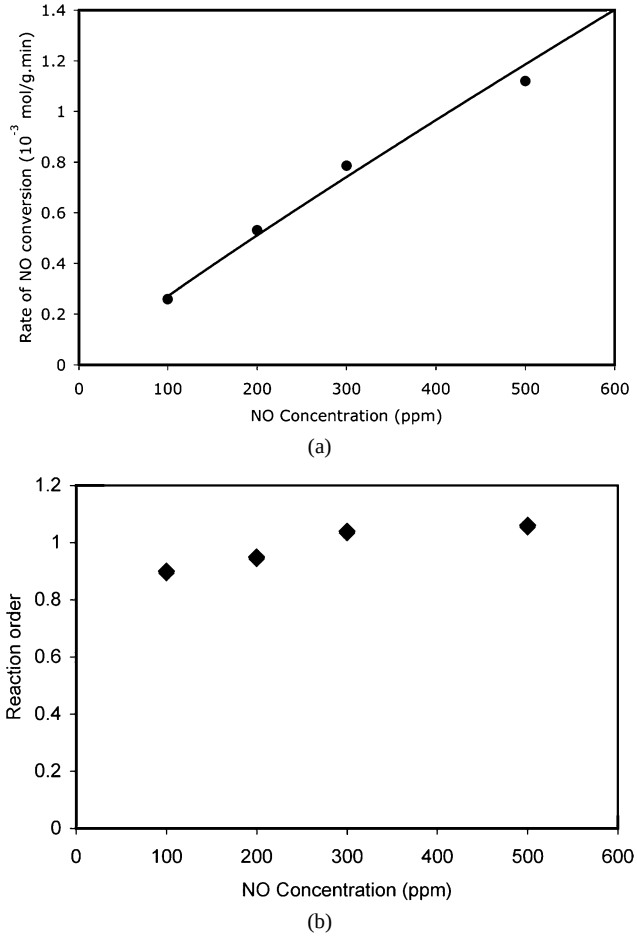

Fig. 9. Dependence of NO conversion rate (upper) and reaction order (lower) on NO concentration on 1%Pd–5%V_2O_5/TiO_2/Al_2O_3 catalyst at 200 °C. Reaction conditions: 5 mg catalyst, [H_2] = 4000 ppm, [CO] = 500 ppm, [O_2] = 5%, He balance, total flow = 500 ml/min.

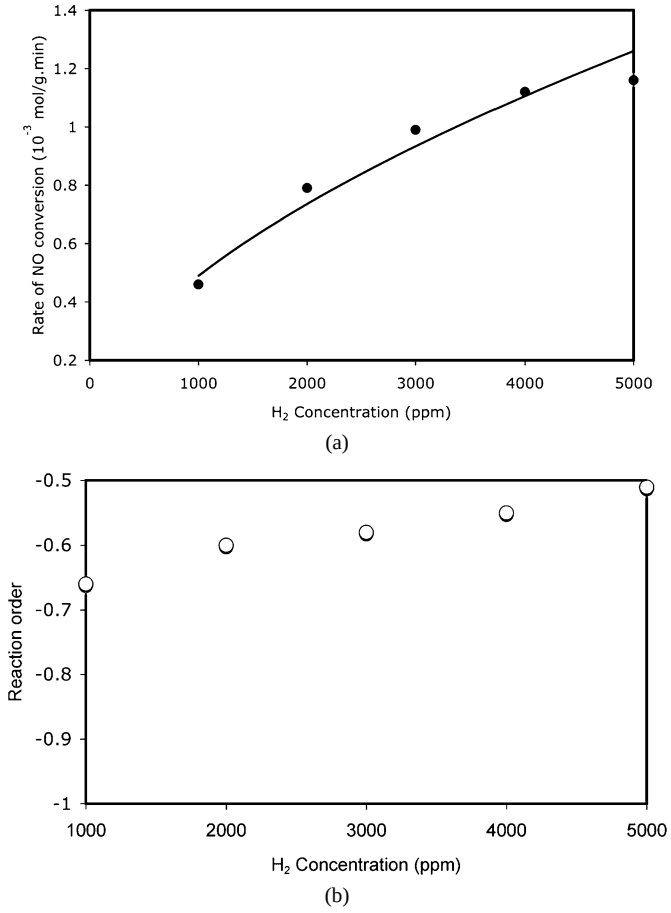

Fig. 10. Dependence of NO conversion rate (upper) and reaction order (lower) on H_2 concentration for 1%Pd–5%V_2O_5/TiO_2/Al_2O_3 catalyst at 200 °C. Reaction conditions: 5 mg catalyst, [NO] = 500 ppm, [CO] = 500 ppm, [O_2] = 5%, He balance, total flow = 500 ml/min.

NO conversion as a function of NO, CO, H_2, and O_2 concentrations are presented in Figs. 9–12. Fig. 9 shows that the rate of NO conversion increased linearly as a function of NO concentration. The reaction rate of NO conversion as a function of reactant concentrations can be expressed as

$$r_{NO} = -k_a[NO]^x[H_2]^y[CO]^z[O_2]^m, \quad (1)$$

where r_{NO} is the SCR rate, k_a is the apparent rate constant, and x, y, z, and m are reaction orders for NO, H_2, CO, and O_2, respectively. According to Fig. 9, the reaction order (x) with respect to NO was 0.92, thus making this reaction close to first order.

Fig. 10 shows that the rate of NO conversion increased with increasing H_2 concentration. The reaction order (y) with respect to the H_2 concentration was calculated as 0.6. In contrast, Fig. 11 shows that the rate of NO conversion decreased with increasing CO concentration. Thus CO inhibits the reaction, due to the competitive adsorption between NO and H_2, as discussed in detail later. The reaction order (z) with respect to CO concentration was calculated to be −0.18. Fig. 12 shows the rate of NO conversion as a function of O_2 concentration (500 ppm NO, 4000 ppm H_2, 500 ppm CO). With an increase in O_2 concentration from 2 to 10%, the NO consumption rate decreased slightly. Low O_2 concentrations (<1%) were not investigated, due to the propensity to form ammonia. The reaction order (m) with respect to O_2 was calculated as −0.04.

According to the foregoing results, the H_2-SCR reaction in the presence of CO and excess O_2 can be considered approximately first order with respect to NO, 0.6-order with respect to H_2, −0.18-order with respect to CO, and −0.04-order with respect to O_2. The rate of NO conversion can be expressed as follows:

$$r_{NO} = -k_a[NO]^{0.92}[H_2]^{0.6}[CO]^{-0.18}[O_2]^{-0.04}. \quad (2)$$

Figs. 9–12 also show the corresponding reaction order for each reactant at different concentrations. For all reactants, the reaction order increased as the concentration was increased.

3.5. Effects of H_2O and SO_2 on the H_2-SCR reaction for the Pd–V_2O_5/TiO_2–Al_2O_3 catalyst

Water vapor, a main component of diesel engine exhaust, often leads to catalyst deactivation. Therefore, resistance of the NO_x abatement catalyst to deactivation by water vapor is a very important factor. Fig. 13 shows the effect of H_2O on SCR activity of the Pd–V_2O_5/TiO_2–Al_2O_3 catalyst. Note that the SCR

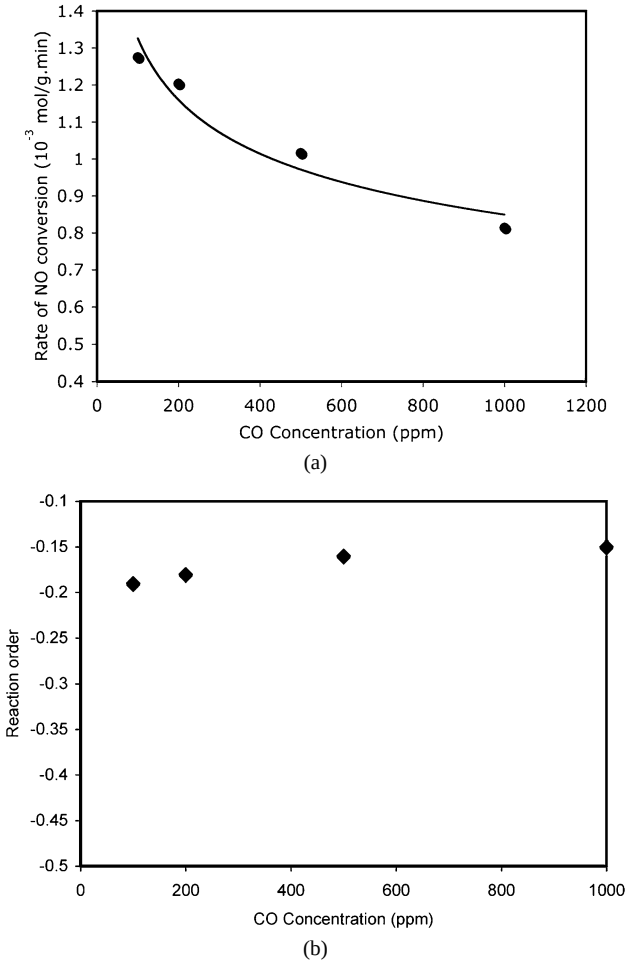

Fig. 11. Dependence of NO conversion rate (upper) and reaction order (lower) on CO concentration for 1%Pd–5%V_2O_5/TiO_2/Al_2O_3 catalyst at 200 °C. Reaction conditions: 5 mg catalyst, [H_2] = 4000 ppm, [NO] = 500 ppm, [O_2] = 5%, He balance, total flow = 500 ml/min.

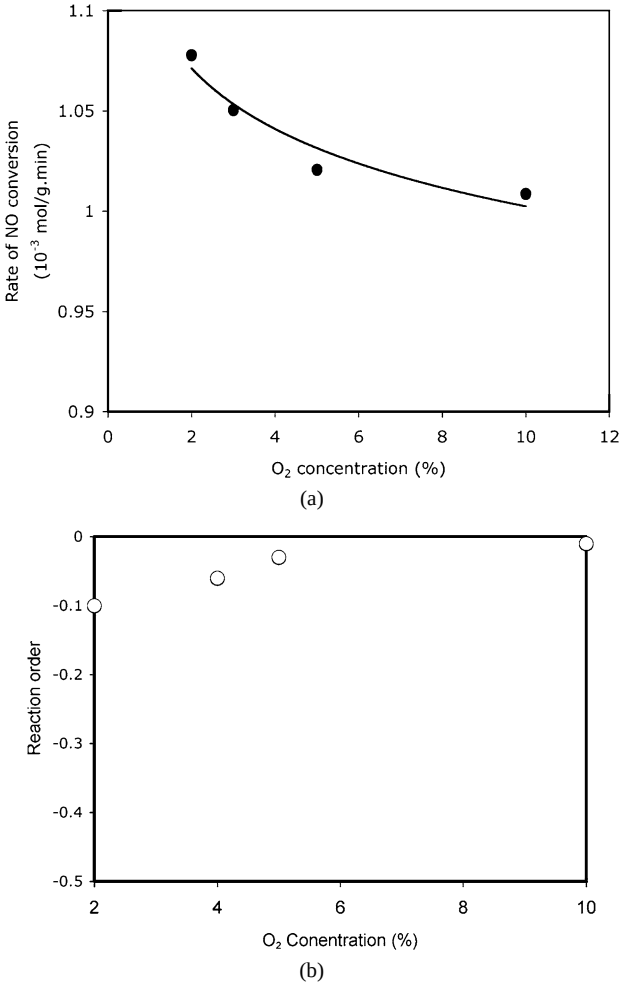

Fig. 12. Dependence of NO conversion rate (upper) and reaction order (lower) on O_2 concentration for 1%Pd–5%V_2O_5/TiO_2/Al_2O_3 catalyst at 200 °C. Reaction conditions: 5 mg catalyst, [H_2] = 4000 ppm, [NO] = 500 ppm, [CO] = 500 ppm, He = balance, total flow = 500 ml/min.

reaction was allowed to stabilize for 1 h at 200 °C before water was added.

The addition of 2.3% H_2O produced a barely detectable decrease in NO conversion. After the water vapor was removed, activity was quickly restored to its original level.

The effect of SO_2 on SCR activity is another important factor in the H_2-SCR reaction due to the presence of very small amounts of sulfur in diesel fuel. Fig. 14 indicates the effect of SO_2 on SCR activity of the Pd–V_2O_5/TiO_2–Al_2O_3 catalyst.

Results indicate that a 20-ppm concentration of SO_2 at 200 °C rapidly decreased the NO conversion rate within the first 2 h of the reaction. Subsequently, the reaction slowly stabilized to yield a 46% conversion (down from 85%) after 4 h. Removal of the SO_2 feed restored the activity to ∼75%.

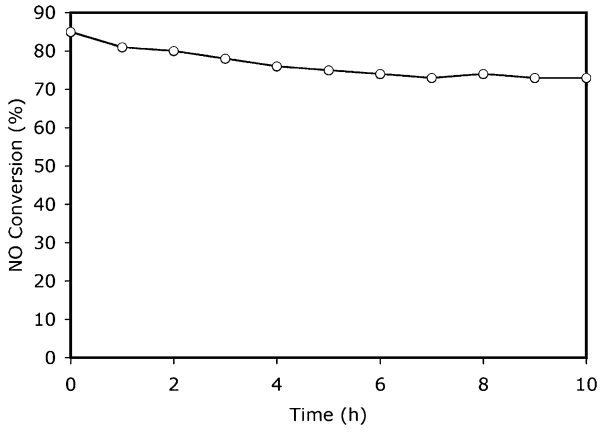

Fig. 13. Effect of H_2O on NO conversion over 1%Pd–5%V_2O_5/TiO_2/Al_2O_3 catalyst at 200 °C. Reaction conditions: 0.05 g catalyst, [H_2] = 4000 ppm, [NO] = 500 ppm, [O_2] 5%, He = balance, [H_2O] = 2.3%, total flow = 500 ml/min.

3.6. FTIR studies

Fig. 15 shows the FTIR spectra obtained at 150, 200, and 240 °C (4000 ppm H_2 + 500 ppm NO + 5% O_2) over the 1%Pd/TiO_2–Al_2O_3 catalyst. At 150 °C, two broad peaks are seen at 1600 and 1300 cm^{-1}. The various bands observed at 1600–1550 and 1300 cm^{-1} may be assigned to the asymmetric and symmetric stretching modes of variously coordinated nitrates [27–30,37]. The bands at 1904 and 1848 cm^{-1} can be attributed to gas phase or weakly adsorbed NO [31–33]. The

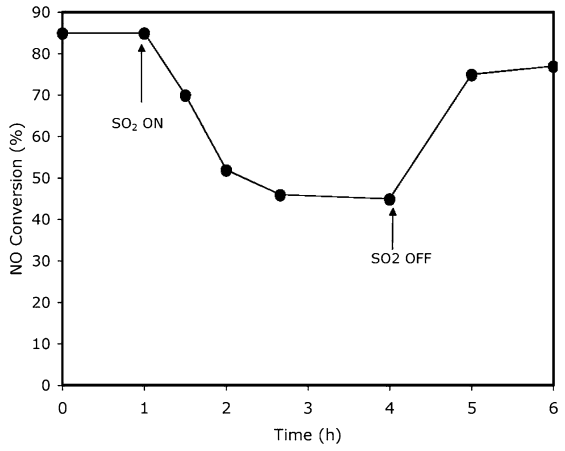

Fig. 14. Effect of SO_2 on NO conversion over 1%Pd–5%V_2O_5/TiO_2/Al_2O_3 catalyst at 200 °C. Reaction conditions: 0.05 g catalyst, [H_2] = 4000 ppm, [NO] = 500 ppm, [O_2] 5%, He = balance, [SO_2] = 20 ppm, total flow = 500 ml/min.

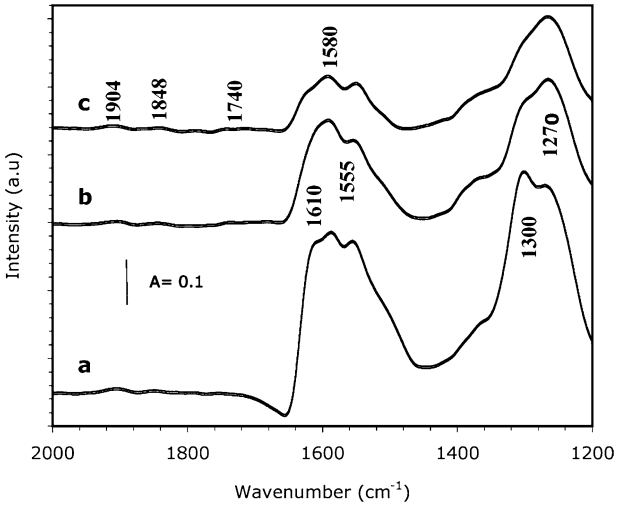

Fig. 15. FTIR spectra obtained at different temperatures in a flow containing 4000 ppm H_2 + 500 ppm NO + 5% O_2 over 1%Pd/TiO_2–Al_2O_3. (a) 150, (b) 200, and (c) 240 °C.

band at 1610 cm^{-1} can be assigned to adsorbed NO_2 [30,31]. The band at 1270 cm^{-1} is attributed to the deformation modes of adsorbed NH_3 [34–36]. Another band at 1620 cm^{-1} due to the deformation modes is barely detected because it is overlapped by the band for nitrate. A very weak band at 1740 cm^{-1} may be assigned to Pd^0–NO [34–36]. All of the bands associated with nitrates and nitrite decreased in intensity as the temperature increased from 150 to 240 °C, whereas the band at 1270 cm^{-1} due to adsorbed NH_3 intensified and dominated at high temperatures.

Fig. 16 shows the corresponding FTIR spectra obtained over 1%Pd–5%V_2O_5/TiO_2–Al_2O_3. At 150 °C (spectrum a of Fig. 16), the bands due to Pd^0–NO (1740 cm^{-1}), gas-phase or weakly adsorbed NO (1904 and 1837 cm^{-1}), NO_2 (1611 cm^{-1}), and nitrate (1583, 1348, and 1300 cm^{-1}) are also observed, similar to the corresponding spectra in Fig. 15. Two new weak bands observed at 1460 and 1680 cm^{-1} were assigned to the symmetric and asymmetric bending modes of

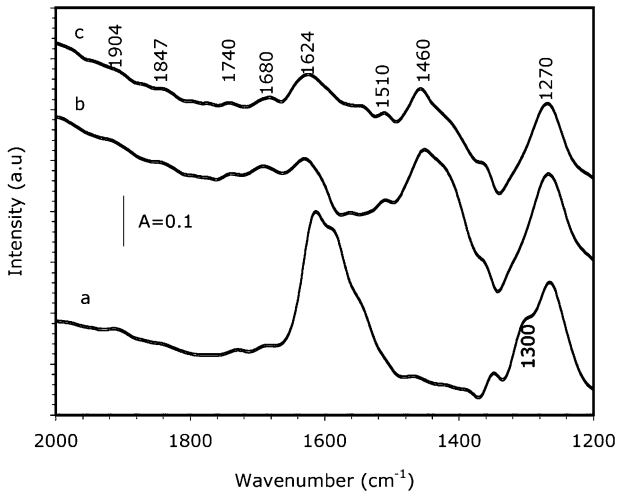

Fig. 16. FTIR spectra obtained at different temperatures in a flow containing 4000 ppm H_2 + 500 ppm NO + 5% O_2 over 1%Pd–5%V_2O_5/TiO_2–Al_2O_3. (a) 150, (b) 200, and (c) 240 °C.

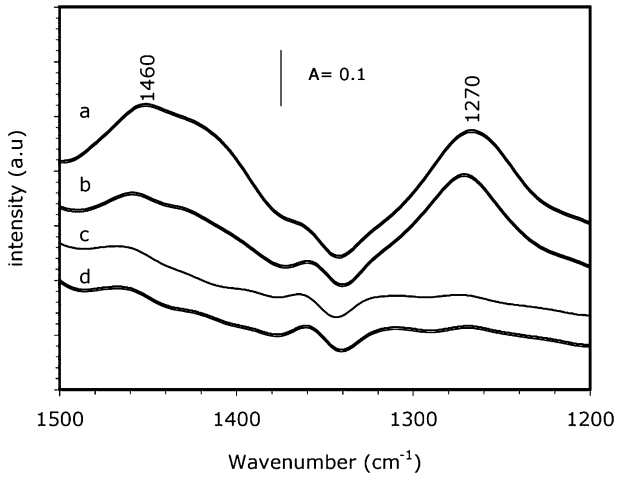

Fig. 17. Changes in the FTIR spectra of NH_3 and NH_4^+ upon switching the gas flow from (4000 ppm H_2 + 500 ppm NO + 5% O_2) to (500 ppm NO + 5% O_2) over 1%Pd–5%V_2O_5/TiO_2–Al_2O_3 catalyst. Time after switching gas flow: (a) 0, (b) 1.5, (c) 3, (d) 10 min.

NH_4^+ [16,17,37–40,43,44]. With increasing temperature, the bands related to nitrates/nitrite decreased significantly, whereas the bands related to ammonium and ammonia first increased (at 200 °C) and then decreased slightly at 240 °C. As the temperature was increased from 150 to 240 °C, two significant differences were observed: (1) The intensity of the bands due to NH_4^+ increased markedly, and (2) a new band at 1510 cm^{-1} due to amide (NH_2) [41,42] was formed. Figs. 15 and 16 show that a significant amount of NH_4^+ was formed at temperatures above 200 °C on 1%Pd–5%V_2O_5/TiO_2–Al_2O_3, which was the reason that the activity was so high at 200 °C on 1%Pd–5%V_2O_5/TiO_2–Al_2O_3 compared with 1%Pd/TiO_2–Al_2O_3.

To study the reactivity of NH_4^+ and NH_3 with NO in the presence of O_2, FTIR spectra (Fig. 17) were obtained over the 1%Pd–5%V_2O_5/TiO_2–Al_2O_3 catalyst at 200 °C after the switch from a feed gas containing 4000 ppm H_2, 500 ppm NO, and 5% O_2 to one containing 500 ppm NO and 5% O_2. After

1.5 min, the band at 1460 cm^{-1} due to NH_4^+ almost disappeared (due to reaction with NO + O_2), whereas the band at 1270 cm^{-1} due to NH_3 exhibited a slight variation. The result indicates that NH_4^+ is more reactive than NH_3 in this SCR reaction; a similar result was reported by Centeno et al. [36], who used a V_2O_5/Al_2O_3 catalyst for the NH_3 SCR reaction. After 10 min, both NH_4^+ and NH_3 peaks disappeared, indicating that both species can react with NO + O_2 at different rates.

4. Discussion

The present work has shown that a 1%Pd–5%$V_2O_5/TiO_2/Al_2O_3$ catalyst offers high NO conversion using H_2 as a reductant in the presence of excess oxygen and at a very high space velocity. Compared with 1%Pd/TiO_2/Al_2O_3, this catalyst also has higher NO reduction activity, as well as a wider operating temperature window.

As shown in Fig. 3, the activity of NO reduction by H_2 in the presence of O_2 is very low at 100 °C, whereas at 150 °C, very high NO conversion was observed on 1%Pd/TiO_2–Al_2O_3 and 1%Pd–5%V_2O_5/TiO_2–Al_2O_3 catalysts. As the reaction temperature was increased, NO conversion decreased on both the 1%Pd/TiO_2–Al_2O_3 and 1%Pd–5%V_2O_5/TiO-Al_2O_3 catalysts but increased on the 5%V_2O_5/TiO_2–Al_2O_3 catalysts. Two distinct maximum NO conversion peaks were observed on the 1%Pd/TiO_2–Al_2O_3 catalyst, as previously reported by Ueda et al. [10] and Lambert et al. [16,17,20]. Conversely, only one maximum NO conversion peak was observed with the 5%V_2O_5/TiO_2–Al_2O_3 and 1%Pd–5%V_2O_5/TiO_2–Al_2O_3 catalysts. Clearly, the modifications to the basic catalyst imposed by the addition of V_2O_5, significantly widened the operating temperature window. A similar trend (Pd/V_2O_5/Al_2O_3) was observed by Macleod and Lambert [22]. Burch and Coleman [24] also reported that adding molybdenum as a promoter resulted in increased NO conversion and N_2 selectivity for the H_2-SCR reaction over a Pt/Al_2O_3 catalyst in the presence of oxygen.

Our results indicate that the low-temperature NO conversion peak was always obtained at the H_2 light-off temperature. This also occurred for the 5%V_2O_5/TiO_2–Al_2O_3 catalyst. Fig. 4 shows that H_2 light-off occurred at a relatively higher temperature for the 1%Pd–5%$V_2O_5/TiO_2/Al_2O_3$ catalyst compared with 1%Pd/TiO_2–Al_2O_3.

It was reported that the low temperature NO conversion peak was related to the adsorption and dissociation of NO and H_2 on palladium metal [21–24,26]. The adsorbed NO dissociates to adsorbed atomic oxygen and atomic nitrogen at above 100 °C [25]. A probable explanation for our results is that V_2O_5 captures some form of reduced nitrogen compound (e.g., NH_3 or a NH_x-type species) that may be formed either on V_2O_5 or abstracted from the nearby Pd sites. A similar reaction pathway was reported by Burch and Coleman [24], who made use of the Mo oxides on a Pt-Mo/Al_2O_3 catalyst and confirmed this trend by FTIR.

A kinetic study carried out at a relatively high temperature (200 °C) demonstrated a decreasing rate of NO conversion with increasing partial pressure of oxygen. This effect was attributed to the competing H_2/O_2 reaction as well as the probable oxidation of Pd. In the absence of oxygen or at very low oxygen partial pressure (<1%), the main products of the H_2-SCR are nitrogen and ammonia [14,20,50]. This investigation focused on oxygen concentrations ⩾2%, to ensure that no ammonia was produced. It became apparent that O_2 concentrations >2% have a negative impact on the reaction. Similar results were reported by Frank et al. [9] for H_2-SCR under lean burn conditions on a Pt–Mo–Co/Al_2O_3 catalyst.

The reaction order with respect to NO was found to be ∼1, which is consistent with a conventional NH_3-SCR reaction. The effect of H_2 concentration was positive. It has been reported that NO dissociation is promoted by atomic hydrogen adsorbed on platinum [45–47], and the same process would be expected to occur on palladium. Hecker and Bell [47] found a positive order dependence of the NO/H_2 reaction on H_2 and proposed that NO dissociation proceeded with the assistance of an adsorbed H atom via the following reaction:

$$NO_{ad} + H_{ad} \rightarrow N_{ad} + OH_{ad}.$$

To elucidate the role of V_2O_5 on the reaction, the FTIR spectra for both V_2O_5-containing and V_2O_5-free catalysts were studied in this work. Fig. 15 shows that over the 1%Pd/TiO_2–Al_2O_3 catalyst, NH_3 species were detected at all temperatures with different intensities. At low temperature (150 °C), nitrate was the dominating species on the surface with a small amount of NH_3 (spectrum (a) in Fig. 15). At higher temperature (>200 °C), bands due to NH_3 dominated. At all the temperatures investigated, no bands due to NH_4^+ were detected. The 1%Pd–5%V_2O_5/TiO_2–Al_2O_3 catalyst gave significantly different spectra (Fig. 16). At 150 °C, nitrate species were prevalent on the surface with a small fraction of NH_3 and a trace amount of NH_4^+ (spectrum (a) of Fig. 16). This is similar to what occurred over the 1%Pd/TiO_2–Al_2O_3 catalyst. When the temperature is increased above 200 °C, the bands due to the nitrate species markedly decreased with the NH_4^+ bands dominating. Thus, the addition of V_2O_5 to the catalyst results in the formation of NH_4^+, which is also the intermediate produced in the NH_3-SCR reaction over V_2O_5/TiO_2 [39] and Fe-ZSM-5 [43,44] type catalysts. The rate of reaction between NH_4^+/NH_3 and NO + O_2 was also investigated with FTIR, shown in Fig. 17. The results illustrate that NH_4^+ is much more reactive than NH_3 in the SCR reaction. The FTIR results indicate a switch of reaction mechanism between 150 and >200 °C. At low temperatures, NO dissociation is believed to be the crucial step dominating the overall reaction; at high temperatures, the NH_3-SCR reaction is the crucial step. Similar results have been discussed previously [9,16,17]. One difference between this system and the standard NH_3-SCR reaction is that in this system some NO dissociation was still present at high temperatures, due to the high level of N_2O formed.

More recently, Macleod et al. [48,49] studied the $H_2/NO/O_2/CO$ reaction on Pd/TiO_2–Al_2O_3 and Pd/Al_2O_3 catalysts and examined the synergy of titania and alumina by DRIFTS, XPS, HREM, and XRD. They concluded that titania was critical for the formation of NCO and for the alumina-promoted hydrolysis of NCO to ammonia. Here we focused on the $H_2/NO/O_2$ reaction on V_2O_5-containing Pd/TiO_2–Al_2O_3 catalyst because

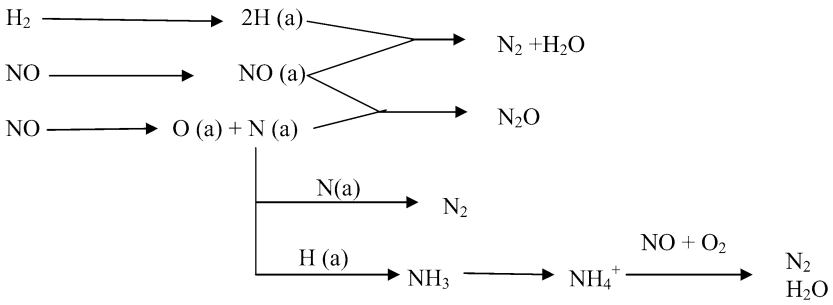

Fig. 18. Reaction scheme of H_2-SCR of NO on $Pd/V_2O_5/TiO_2–Al_2O_3$ catalysts.

of the negative effect of CO found in this study. In the present study, a mechanism of H_2-SCR of NO on $Pd/V_2O_5/TiO_2–Al_2O_3$ was proposed (Fig. 18). The reaction starts with the dissociation of H_2 into H atoms and the dissociation of NO into N and O atoms on the Pd metal surface. N_2 was produced by the reaction of N to another N, whereas N_2O was produced by the reaction of N to adsorbed NO. The fact that the reaction order of NO was nearly first order indicates that NO dissociation and adsorbed NO were rapidly equilibrated with gaseous NO. NH_3 was produced by consecutive hydrogenation of N, and then the formed NH_3 reacted with (possibly involving spillover) the Brönsted acid sites to form NH_4^+. On the Brönsted acid sites of the catalyst, N_2 was produced by ammonia and ammonium reacted to NO and O_2 (as in the ammonia-SCR reaction studied extensively in the literature). From this mechanism, it can be concluded that this reaction is basically a bifunctional reaction mechanism on Pd and support. Based on the activity results (Fig. 3), at low temperature, NO conversion was related mainly to the Pd metal, because very low NO conversion was reached on Pd-free samples. In the high-temperature range (>240 °C), NO conversion did not differ much on Pd-containing and Pd-free samples, which means that the supports including V_2O_5 have played a significant role. Based on different NO conversions on $Pd/V_2O_5/TiO_2–Al_2O_3$ and $V_2O_5/TiO_2–Al_2O_3$, it can be concluded that at 150 °C, most of the NO conversion occurred on Pd alone; at 240 °C, most of the NO conversion occurred on supports; and at 200 °C, nearly half of the NO conversion occurred on Pd alone and the supports.

5. Conclusion

The catalytic reduction of NO with hydrogen in the presence of excess oxygen was studied over Pd-based catalysts for NO_x abatement applications in diesel engine exhaust. A high steady-state conversion of NO (>80%) is achieved at reaction temperatures in the range 140–250 °C over the $1\%Pd–5\%V_2O_5/TiO_2–Al_2O_3$ catalyst. Adding V_2O_5 to the initial $1\%Pd/TiO_2/Al_2O_3$ catalyst increases NO conversion, especially at temperatures around 200 °C. The reaction order is nearly first order with respect to NO, 0.6-order with respect to H_2, and −0.18-order with respect to CO. Increasing the O_2 concentration from 2 to 10% produced only a slight decrease in NO conversion. FTIR studies showed significant NH_4^+ formation above 200 °C over the V_2O_5-containing catalyst, compared with nearly no NH_4^+ observed on the V_2O_5-free sample. The NH_4^+ specie was more reactive than NH_3 in these SCR reactions, to which the higher activity of the $1\%Pd–5\%V_2O_5/TiO_2–Al_2O_3$ catalyst was attributed.

Acknowledgments

This work was supported by Tenneco Automotive, Exhaust Engineering Center.

References

[1] L.R. Raber, Chem. & Eng. News April 14 (1997) 10.
[2] H. Bosch, F. Janssen, Catal. Today 2 (1988) 369.
[3] G. Busca, L. Lietti, G. Ramis, F. Berti, Appl. Catal. B 18 (1998) 1.
[4] R.M. Heck, R.J. Farrauto, Catalytic Air Pollution Control, Van Nostrand Reinhold, New York, 1995.
[5] M. Koebel, M. Elsener, M. Kleemann, Catal. Today 59 (2000) 335.
[6] M. Koebel, M. Elsener, T. Marti, Combust. Sci. Tech. 121 (1996) 85.
[7] J.H. Baik, S.D. Yim, I.S. Nam, Y.S. Mok, J.H. Lee, B.K. Cho, S.H. Oh, Top. Catal. 30 (2004) 37.
[8] K. Yokota, M. Fukui, T. Tanaka, Appl. Surf. Sci. 121/122 (1997) 273.
[9] B. Frank, G. Emig, A. Renken, Appl. Catal. B 19 (1998) 45.
[10] A. Ueda, N. Takayuki, A. Masashi, T. Kobayashi, Catal. Today 45 (1998) 135.
[11] R. Burch, M.D. Coleman, Appl. Catal. B 23 (1999) 115.
[12] C.N. Costa, V.N. Stathopoulos, V.C. Belessi, A.M. Efstathiou, J. Catal. 197 (2001) 350.
[13] K.C. Taylor, R.L. Klimisch, J. Catal. 30 (1973) 478.
[14] T.P. Kobylinski, B.W. Taylor, J. Catal. 33 (1974) 376.
[15] W. Dabil, S.J. Gentry, H.B. Holland, A. Jones, J. Catal. 53 (1978) 164.
[16] N. Macleod, R.M. Lambert, Appl. Catal. B 35 (2002) 269.
[17] N. Macleod, R.M. Lambert, Catal. Commun. 3 (2002) 61.
[18] Y.-W. Lee, E. Gulari, Catal. Commun. 5 (2004) 499.
[19] T. Nanba, K. Sugawara, S. Masukawa, J. Uchisawa, A. Obuchi, Ind. Eng. Chem. Res. 44 (2005) 3426.
[20] J.H. Jones, J.T. Kummer, K. Otto, M. Shelef, E. Weaver, Environ. Sci. Tech. 5 (1971) 791.
[21] N. Macleod, R. Cropley, R.M. Lambert, Catal. Lett. 86 (2003) 69.
[22] N. Macleod, R.M. Lambert, Catal. Lett. 90 (2003) 111.
[23] B. Wen, Fuel 81 (2002) 1841.
[24] R. Burch, M.D. Coleman, J. Catal. 208 (2002) 435.
[25] M. Slinko, T. Fink, T. Löher, H.H. Madden, S.J. Lombardo, R. Imbihl, G. Ertl, Surf. Sci. 264 (1992) 157.
[26] R. Burch, P.J. Millington, A.P. Walker, Appl. Catal. B 4 (1994) 65.
[27] W.S. Kijlstra, D.S. Brand, E.K. Poels, A. Bliek, J. Catal. 171 (1997) 208.
[28] F.C. Meunier, J.P. Breen, V. Zuaniuk, M. Olsson, J.R.H. Ross, J. Catal. 187 (1999) 493.
[29] S. Kameoka, Y. Ukisu, T. Miyadera, Phys. Chem. Chem. Phys. 2 (2000) 367.
[30] J. Laane, J.R. Ohlsen, Prog. Inorg. Chem. 28 (1986) 465.
[31] K. Hadjiivanov, H. Knözinger, Phys. Chem. Chem. Phys. 2 (2000) 2803.

[32] A. Martínez-Arias, J. Soria, J.C. Conesa, X.L. Seoane, A. Arcoya, R. Cataluña, J. Chem. Soc., Faraday Trans. 91 (1995) 1679.
[33] G. Ramis, L. Yi, G. Busca, Catal. Today 28 (1996) 373.
[34] G. Ramis, G. Busca, V. Lorenzelli, P. Forzatti, App. Catal. 64 (1990) 243.
[35] G. Ramis, L. Yi, G. Busca, M. Turco, E. Totur, R.J. Willy, J. Catal. 157 (1998) 523.
[36] M.A. Centeno, I. Carrizosa, J.A. Odriozola, Appl. Catal. B 19 (1988) 67.
[37] K.I. Hadjiivanov, Catal. Rev. Sci. Eng. 42 (2002) 71.
[38] R.Q. Long, R.T. Yang, J. Catal. 196 (2000) 73.
[39] N.Y. Topsøe, H. Topsøe, J.A. Dumesic, J. Catal. 151 (1995) 226.
[40] H. Schneider, S. Tschudin, M. Schneider, A. Wokaun, A. Baiker, J. Catal. 147 (1994) 5.
[41] W.S. Kijlstra, D.S. Brands, H.I. Smit, E.K. Poels, A. Bliek, J. Catal. 219 (1997) 171.
[42] G. Qi, R.T. Yang, J. Phys. Chem. B 108 (2004) 15738.
[43] G. Qi, R.T. Yang, Appl. Catal. B 60 (2005) 13.
[44] G. Qi, R.T. Yang, Appl. Catal. A 287 (2005) 25.
[45] M. Uchida, A.T. Bell, J. Catal. 60 (1979) 204.
[46] G. Pirug, H.P. Bonzel, J. Catal. 50 (1977) 64.
[47] W.C. Hecker, A.T. Bell, J. Catal. 92 (1985) 247.
[48] N. Macleod, R. Cropley, J.M. Keel, R.M. Lambert, J. Catal. 221 (2004) 20.
[49] N. Macleod, R.M. Lambert, Appl. Catal. B 46 (2003) 483.
[50] R. Burch, A.A. Shestov, J.A. Sullivan, J. Catal. 188 (1999) 69.